arXiv:hep-ph/0209262v4 12 Dec 2002

ANL-HEP-PR-02-054
EFI-02-94
FERMILAB-Pub-02/215-T
hep-ph/0209262

Elastic Scattering and Direct Detection of Kaluza–Klein Dark Matter

Géraldine Servant [a,b] and Tim M.P. Tait [a,c]

[a] *High Energy Physics Division, Argonne National Laboratory, Argonne, IL 60439*
[b] *Enrico Fermi Institute, University of Chicago, Chicago, IL 60637*
[c] *Fermi National Accelerator Laboratory, P.O. Box 500, Batavia, IL 60510*

servant@theory.uchicago.edu, tait@fnal.gov

Abstract

Recently a new dark matter candidate has been proposed as a consequence of universal compact extra dimensions. It was found that to account for cosmological observations, the masses of the first Kaluza-Klein modes (and thus the approximate size of the extra dimension) should be in the range 600-1200 GeV when the lightest Kaluza-Klein particle (LKP) corresponds to the hypercharge boson and in the range 1 - 1.8 TeV when it corresponds to a neutrino. In this article, we compute the elastic scattering cross sections between Kaluza-Klein dark matter and nuclei both when the lightest Kaluza-Klein particle is a KK mode of a weak gauge boson, and when it is a neutrino. We include nuclear form factor effects which are important to take into account due to the large LKP masses favored by estimates of the relic density. We present both differential and integrated rates for present and proposed Germanium, NaI and Xenon detectors. Observable rates at current detectors are typically less than one event per year, but the next generation of detectors can probe a significant fraction of the relevant parameter space.

1 Introduction

Recently a new type of dark matter candidate has been proposed, consisting of stable Kaluza-Klein (KK) modes of ordinary standard model particles allowed to propagate in one or more compact extra dimensions [1, 2, 3]. Under reasonably mild assumptions about the nature of the UV completion, a five dimensional (5d) theory with orbifold boundary conditions has a lightest Kaluza-Klein particle (LKP) which is stable, and thus would be present as a cold relic in the universe today. If one further assumes that the LKP is a neutral, non-baryonic particle, it has all of the properties required of a well-motivated weakly interacting massive particle (WIMP), and what remains is to determine the relevant range of masses and other parameters needed in order to correctly account for cosmological observations, and to determine the sensitivity of current and future dark matter searches to detect it either directly or indirectly.

Models with compact extra dimensions possess a very rich phenomenology and have attracted much attention lately. Fields which are permitted to propagate in the extra dimensions appear to a low energy observer as a tower of increasingly massive particles, each with identical spin and charge. The massive states are in fact modes of the fields which carry (quantized) momentum in the extra dimensions, and thus the spacing of the tower is roughly $1/R$, the inverse size of the extra dimensions. The ordinary particles of everyday experience are identified with the "zero modes", carrying zero momentum in the compact directions. Models with extra dimensions may be classified according to which fields are allowed to propagate in extra dimensions. In brane world models, only gravitational fields can propagate in extra dimensions and therefore have KK excitations. There are other interesting models where standard model gauge bosons live in the bulk as well while standard model matter fermions are still confined on a 3-dimensional surface. And finally, there exist models –the so-called models with *Universal Extra Dimensions* (UED) [4]– in which all standard model fields have KK modes. These three classes of models have very distinct phenomenology. UED models are the only models with extra dimensions to have a stable KK particle because of a discrete symmetry (KK parity) which is remnant of the higher dimensional Poincaré invariance. Under KK parity, all even mode-number particles (including the zero modes) are even, while the odd modes are odd. This has the desired consequence that the lightest odd mode must be stable. If this lightest KK Particle is neutral and weakly interacting, it provides a cold dark matter candidate.

Having fermions in extra dimensions requires further assumptions about the nature of the compact dimensions. Generally, from the four dimensional point of view, a fermion in higher dimensions will not have chiral interactions, a necessary ingredient of any electroweak theory. This may be addressed in the UED context by imposing orbifold boundary conditions which project out the zero modes of the unwanted degrees of freedon responsible for vector-like interactions. For five dimensions, this can be accomplished by identifying the coordinate of the extra dimension y with $-y$, folding the circle S^1 onto the line S^1/Z_2. In six dimensions, starting from a 2-torus T^2, one can identify either points related by a rotation of 180 degrees (T^2/Z_2) or by 90 degrees (T^2/Z_4). One can similarly consider

cases in even more dimensions, but we will restrict our discussion, for simplicity, to the five or six dimensional cases. Having imposed the orbifold in order to recover a chiral low energy theory, it can be shown [5] that the needed boundary conditions imply that there are terms in the Lagrangian which live on the fixed points of the orbifold transformation. In five dimensions, these are the points on the boundaries of the extra dimension. These boundary terms cannot be computed in terms of other parameters without knowing the UV completion of the theory. Consequently they must instead be treated as parameters of the UED model. We expect that the masses of the first level KK modes should be of order $1/R$, but will have corrections from the boundary terms which will in general be different for different fields.

The most interesting cases for dark matter are when the boundary terms are such that the LKP is a KK mode of either a neutrino, a neutral Higgs or a neutral weak gauge boson. In this work we focus on the neutrino and gauge boson possibilities. Because of electroweak symmetry-breaking, the KK towers of the hypercharge boson B and the neutral $SU(2)$ boson W_3 mix. The mass matrix for the first level KK modes (in five dimensions) may be expressed in the ($B^{(1)}$, $W_3^{(1)}$) basis,

$$\begin{pmatrix} \frac{1}{R^2} + \frac{1}{4}g_1^2v^2 + \delta M_1^2 & \frac{1}{4}g_1g_2v^2 \\ \frac{1}{4}g_1g_2v^2 & \frac{1}{R^2} + \frac{1}{4}g_2^2v^2 + \delta M_2^2 \end{pmatrix}, \tag{1}$$

where R is the size of the extra dimension, v is the Higgs vacuum expectation value, g_1 and g_2 are the gauge couplings, and δM_i^2 are the boundary terms. If the boundary terms are induced radiatively, they should be proportional to the gauge couplings and $1/R^2$. Thus, for $1/R \gg v$, the matrix is rather close to diagonal, and since $g_1 < g_2$ we can expect that the lighter particle is well-approximated as being entirely $B^{(1)}$. Thus, in this case the LKP is a massive neutral vector particle which couples to matter proportionally to g_1 times the hypercharge.

In Ref. [1], we determined the relic density for the LKP when it is either a KK mode of a neutrino ($\nu^{(1)}$) or of a neutral gauge boson ($B^{(1)}$). As seen above, these represent natural candidates when terms confined to the orbifold fixed points are taken to arise radiatively[1] [6], as opposed to being present at tree-level [7]. A variety of co-annihilation channels were included, with a range of mass splittings between the LKP and heavier first tier KK modes, and the conclusion is that in order to correctly account for the observed density of dark matter, the LKP masses should lie in the ranges 600 to 1200 GeV for $B^{(1)}$ and 1000 and 1800 GeV for $\nu^{(1)}$. We also noted that for a six dimensional (6D) orbifold T^2/Z_2, these mass ranges are lowered by approximately a factor of $\sqrt{2}$. Under our assumption of small boundary terms, the LKP mass corresponds to the inverse radius of the compact dimension and we expect all first level KK modes to have masses of this order. The range relevant for dark matter is particularly tantalizing because it lies just above the current bounds from high energy colliders [4][2]. Given the very large number of

[1] $B^{(1)}$ is indeed the LKP when assuming vanishing boundary terms at the cut-off scale. Note that this kind of prescription is similar to the choice of universal soft SUSY breaking masses at the GUT scale in susy models.

[2] The possibility of an extra dimension at a TeV was first examined in [8].

currently running or planned experiments devoted to both direct and indirect searches for WIMPs, the detectability of KK dark matter is an interesting question. Indirect detection issues have recently started to be investigated [9, 10, 11].

Direct detection of a weakly interacting massive particle typically involves searching for the rare scattering of the WIMP with a nucleus in a detector. As a result of the interaction, the nucleus recoils with some energy, which can be read out as a signal [12]. The distribution of recoil energies is a function of the masses of the WIMP and the nucleus, and (because the scattering length for heavy WIMPs is typically of the same order as the size of the nucleus) the nuclear wave function. The lightest supersymmetric particle (LSP) is a typical Majorana fermion WIMP with mass on the order of 100 GeV, and theoretical predictions for its interactions at modern dark matter detectors have reached a high level of sophistication. In Ref. [9], computations for the cross sections of $B^{(1)}$ scattering with nucleons were performed and prospects for direct detection at present experiments were presented. In contrast with Supersymmetric WIMPs, predictions depend only on three parameters: The LKP mass, the mass difference between the LKP and the KK quarks (assuming all flavors and chiralities of first level KK quarks are degenerate in mass) and the "zero mode" Higgs mass. It is clear that present experiments can only probe KK masses below 400 GeV as soon as the mass splitting between the LKP and KK quarks is larger than five percents (as is found in [6]). On the other hand, masses below 300 GeV are already excluded by collider constraints [4]. And in any case, masses below 400 GeV are in conflict with the mass range predicted from our relic density calculation [1]. Therefore, we wish to investigate detection prospects for masses above 400 GeV and ask: Which planned experiment will be able to probe the relevant parameter space of the LKP? To answer this question, we need to go beyond the wimp-nucleon cross section calculation and compute the event rate for a given detector. This requires to include the nuclear form factor. In the current article we expand upon the results of Ref. [9], deriving realistic estimates for event rates at modern dark matter detectors, including nuclear wave function effects and examining differential rates in the nuclear recoil energy as well as integrated ones. We find that the event rate is somewhat smaller than for the usual LSP neutralino WIMP with mass around 100 GeV and that in order to see at least several events per year, heavy (> 100 kg) detectors are needed.

This article is organized as follows. In section II we review the kinematics of direct detection of WIMPs. In section III, we present the analysis in the case where the LKP is the first KK state of the neutrino, finding that it should most likely have already been observed by CDMS or EDELWEISS, and thus is excluded. Section IV is devoted to the more interesting case of $B^{(1)}$. Our predictions for the differential and integrated event rates expected in Germanium, Sodium–Iodide and Xenon detectors are presented in section V. We reserve section VI for our conclusions and outlook.

2 Kinematics of WIMP Detection

In this section we briefly review the general kinematics of WIMP-nucleus scattering. The number of events per unit time and per unit detector mass is,

$$dR = \frac{\rho}{mM}\frac{d\sigma}{d|\mathbf{q}|^2}d|\mathbf{q}|^2 v f(v) dv, \tag{2}$$

where m is the WIMP mass and ρ its mass density in our solar system[3], and M is the mass of the target nucleus. $f(v)$ is the distribution of WIMP velocities relative to the detector, $\mu \equiv mM/(m+M)$ is the reduced mass, q^μ is the momentum transfer four-vector whose magnitude is $|\mathbf{q}|^2 = 2\mu^2 v^2(1-\cos\theta)$ in terms of θ, the scattering angle in the center of momentum frame. $|\mathbf{q}|^2$ is related to the recoil kinetic energy E_r deposited in the detector (in the lab frame) by $E_r = |\mathbf{q}|^2/2M$. For $m \gg M$ as is the case for LKP WIMPs with masses of order 1 TeV, E_r is typically 30–50 keV depending on the nucleus target (but it can be much larger for WIMPs with velocities close to the galactic escape velocity). Eq. (2) may be thus rewritten

$$\frac{dR}{dE_r} = \frac{2\rho}{m}\frac{d\sigma}{d|\mathbf{q}|^2} v f(v) dv, \tag{3}$$

in which $|\mathbf{q}|^2$ should be regarded as a function of E_r as indicated above. The differential cross section can be expressed in terms of the cross section at zero momentum transfer σ_0 times a nuclear form factor [14],

$$\frac{d\sigma}{d|\mathbf{q}|^2} = \frac{\sigma_0}{4\mu^2 v^2} F^2(|\mathbf{q}|), \tag{4}$$

where $F^2(|\mathbf{q}|)$ is a function normalized to one at $|\mathbf{q}|^2 = 0$ which includes all relevant nuclear effects and must be determined either directly from measurements of nuclear properties or estimated from a nuclear model, and σ_0 contains the model-dependent factors for a specific WIMP. The rate is obtained by integrating over all possible incoming velocities of the WIMP:

$$\frac{dR}{dE_r} = \frac{\sigma_0 \rho}{2m\mu^2} F^2(|\mathbf{q}|) \int_{v_{min}}^{v_{max}} \frac{f(v)}{v} dv, \tag{5}$$

where $v_{max} \simeq 650$ km/s, the galactic escape velocity. To determine v_{min} we use the relation between the WIMP energy E and the recoil energy E_r

$$E = \frac{2E_r}{1-\cos\theta}\frac{(m+M)^2}{4mM} \rightarrow E_{min} = E_r \frac{(m+M)^2}{4mM}, \tag{6}$$

$$v_{min} = (2E_{min}/m)^{1/2} = \sqrt{\frac{E_r M}{2\mu^2}}. \tag{7}$$

[3]In our numerical results, we identify ρ with the local (in our galaxy) dark matter density of canonical value $\rho \sim 0.3$ GeV/cm^3 [13] *i.e.* we assume a homogeneous halo of our galaxy. This assumption is not obvious. In addition, estimates of the local density of dark matter in our galaxy is subject to considerable uncertainty and model-dependance. We should then keep in mind that local over- or underdensities could easily change the expected detection rate by a significant amount.

Assuming a Maxwellian velocity distribution for the WIMPs and including the motion of the Sun and the Earth one obtains [14],

$$\int_{v_{min}}^{\infty} \frac{f(v)}{v} dv = \frac{1}{2v_E} \left[\mathrm{erf}\left(\frac{v_{min} + v_E}{v_0} \right) - \mathrm{erf}\left(\frac{v_{min} - v_E}{v_0} \right) \right], \tag{8}$$

where v_E is the relative motion of the observer on the Earth to the sun (and thus shows an annual modulation), and v_0 is the mean relative velocity of the sun relative to the galactic center[4]. Thus, the final formula for the measured differential event rate is,

$$\frac{dR}{dE_r} = \frac{\sigma_0 \rho}{4 v_E m \mu^2} F^2(|\mathbf{q}|) \left[\mathrm{erf}\left(\frac{v_{min} + v_E}{v_0} \right) - \mathrm{erf}\left(\frac{v_{min} - v_E}{v_0} \right) \right]. \tag{9}$$

The total event rates per unit detector mass and per unit time will depend on the range of energies to which the detector is sensitive. Thus, the actual observed rate, modulo experimental efficiencies, will be given by dR/dE_r integrated over the appropriate range of energy for a given experiment.

Our task will now be to compute σ_0 and to combine it with the correct form factor $F^2(|\mathbf{q}|)$ in cases where the WIMP is $\nu^{(1)}$ or $B^{(1)}$. To compute σ_0, we must evaluate the effective WIMP interaction with nuclei by evaluating the matrix elements of the nucleon operators in a nuclear state. This in turn is determined from WIMP interactions with quarks and gluons evaluated in nucleon states. Traditionally, one differentiates between two very different types of WIMP-nucleon interactions- *spin-dependent* interactions and *scalar* interactions.

Scalar interactions are coherent between nucleons in the nucleus, and the form factor is thus the Fourier transform of the nucleon density. The commonly used form (identical, in the limit of low momentum transfer, to the one derived from a *Woods–Saxon* parametrization of the nuclear density [14, 15]) is :

$$F^2(|\mathbf{q}|) = \left(\frac{3 j_1(q R_1))}{q R_1} \right)^2 e^{-(qs)^2}, \tag{10}$$

where $R_1 = \sqrt{R^2 - 5s^2}$ and $R \sim 1.2$ fm $\mathrm{A}^{1/3}$ with A the nuclear mass number, $s \sim 1$ fm and j_1 is a spherical Bessel function,

$$j_1(q r_n) \;\; = \;\; \frac{\sin[q r_n] - q r_n \cos[q r_n]}{(q r_n)^2}. \tag{11}$$

An axial-vector interaction leads to interactions between the WIMP spin and nucleon spin. In this case one must evaluate the matrix elements of nucleon spin operators in the nuclear state. The form factor is typically written as [14, 15] ,

$$F^2(|\mathbf{q}|) = \frac{S(|\mathbf{q}|)}{S(0)}, \tag{12}$$

[4]Together with ρ, note that v_0 is another crucial quantity in both direct and indirect methods of dark matter detection which is subject to significant uncertainties.

where,

$$S(|\mathbf{q}|) = a_0^2 S_{00}(|\mathbf{q}|) + a_1^2 S_{11}(|\mathbf{q}|) + a_0 a_1 S_{01}(|\mathbf{q}|), \quad (13)$$

$$a_0 = a_p + a_n, \quad a_1 = a_p - a_n, \quad (14)$$

where the first term is the iso-scalar contribution, the second one is the iso-vector contribution and the last one is the interference term between the two. The S_{ij} are obtained from nuclear calculations. a_p and a_n reflect the spin-dependent WIMP interactions and average spins for neutrons and protons in the nucleus and will be defined below.

3 Direct Detection of $\nu^{(1)}$

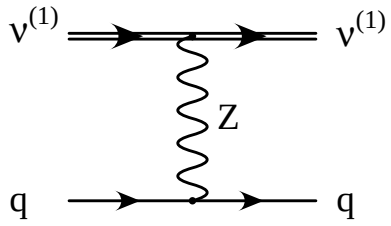

Figure 1: Leading Feynman graph for effective $\nu^{(1)}$-quark scattering through the exchange of a zero-mode Z gauge boson.

For our first example, we consider the KK neutrino, $\nu^{(1)}$. This is almost a case which has been considered previously [12], the only difference being that the KK neutrino has vector-like weak interactions. In the non relativistic limit where $q^2 \ll m_Z^2$, we have an effective four-fermion contact interaction (Fig. 1),

$$\frac{-ie^2}{4\sin^2\theta_W m_W^2}\left[\overline{u}_\nu \gamma^\mu u_\nu\right]\left(\left(g_R^q + g_L^q\right)\left[\overline{q}(x)\gamma_\mu q(x)\right] + \left(g_R^q - g_L^q\right)\left[\overline{q}(x)\gamma_\mu\gamma_5 q(x)\right]\right), \quad (15)$$

where we have explicitly included the Z couplings to $\nu^{(1)}$,

$$g_R^{\nu^{(1)}} = g_L^{\nu^{(1)}} = \frac{e}{2\sin\theta_W\cos\theta_W}, \quad (16)$$

and the g_L^q and g_R^q are the left- and right-handed quark interactions with the Z boson,

$$g^q = T_3^q - Q_q \sin^2\theta_W. \quad (17)$$

Thus we see that the effective interaction includes both a coupling to the vector and the axial vector quark currents. When evaluating the WIMP-nucleon cross section, this will be summed over all flavors of quarks and will involve matrix elements $\langle\overline{q}\gamma_\mu q\rangle$ and $\langle\overline{q}\gamma_\mu\gamma_5 q\rangle$, where the expectation values are to be understood as refering to nucleon states.

The WIMPs are highly non-relativistic, and thus only the time-component of the vector $\overline{u}_\nu \gamma^\mu u_\nu$ is appreciable. However, the expectation value $\langle \overline{q}\gamma_0\gamma_5 q\rangle \simeq 0$ [15], and we are left with only the time-component of the vector interaction. This illustrates the predominant difference between $\nu^{(1)}$ and a typical massive Dirac neutrino WIMP - the absence of spin-dependent interactions. However, since the spin-dependent contribution is usually sub-dominant to the scalar interaction, the resulting cross sections remain comparable.

At the quark level, the effective interaction has the form,

$$b_q \left[\overline{u}_\nu \gamma^\mu u_\nu\right] \left[\overline{q}(x)\gamma_\mu q(x)\right], \tag{18}$$

where,

$$b_q \;=\; \frac{e^2}{4\sin^2\theta_W m_W^2}\left[T_3^q - 2Q_q \sin^2\theta_W\right]. \tag{19}$$

The matrix element $\langle \overline{q}\gamma^0 q\rangle = \langle q^\dagger q\rangle$ simply counts valence quarks in the nucleon, and so the nucleon WIMP couplings are,

$$b_p \;=\; 2b_u + b_d = \frac{G_F}{\sqrt{2}}\left(1 - 4\sin^2\theta_W\right), \tag{20}$$

$$b_n \;=\; 2b_d + b_u = -\frac{G_F}{\sqrt{2}}, \tag{21}$$

for the proton and neutron, respectively. The numerical accident that $\sin^2\theta_W \simeq 1/4$ renders the coupling to protons very small. The vector interactions are coherent, and thus we have for the WIMP-nucleus coupling, $b_N = Zb_p + (A-Z)b_n$. Thus,

$$\sigma_0 \;=\; \frac{\mu^2 G_F^2}{2\pi}\left[(1 - 4\sin^2\theta_W)Z - (A-Z)\right]^2 \tag{22}$$

and the form factor entering in the differential cross section $d\sigma/d\mathbf{q}^2$ is given by (10).

It is well-known that the mass of Dirac neutrinos is strongly constrained by elastic scattering experiments such as CDMS [16] and EDELWEISS [17]. The exclusion plots are presented in the m-σ_n plane where m is the mass of the dark matter candidate and σ_n is the scattering cross section per nucleon. It is related to σ_0 by,

$$\sigma_n \;=\; \sigma_0 \frac{m_n^2}{\mu^2 A^2} \tag{23}$$

m_n being the mass of the nucleon. For ^{73}Ge, and $m \gg M$, we find $\sigma_n \sim 2\times 10^{-39}$ cm$^2 \sim 2\times 10^{-3}$ pb. Given that CDMS and EDELWEISS did not see any events, a WIMP with this cross section must have a mass $\gtrsim 50$ TeV. This means that in order to have escaped detection, $\nu^{(1)}$ would have to have masses more than ten times larger than the range of masses for which result in the correct dark matter relic density. While one might imagine that coannihilation in various channels could push up the favored $\nu^{(1)}$ masses by

a few TeV , it seems unlikely that the relic density calculation could favor masses above 10 TeV.

To conclude this section, the KK neutrino seems to be ruled out as a dark matter candidate at least in the minimal UED model where the mass window prediction from the relic density calculation is in conflict with direct detection experiments. Let us therefore now concentrate on the $B^{(1)}$ LKP candidate.

4 Direct Detection of $B^{(1)}$

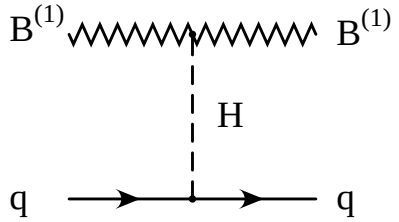

Figure 2: Leading Feynman graph for effective $B^{(1)}$-quark scattering through the exchange of a zero-mode Higgs boson.

$B^{(1)}$ can interact elastically with a quark by exchanging a KK quark in the s- and t-channel or by t-channel Higgs exchange. The amplitude for scattering between quarks and $B^{(1)}$ mediated by Higgs exchange (Figure 2) is,

$$\mathcal{M}_h = -i\gamma_q\, \epsilon^*_\mu(p'_B)\, \epsilon^\mu(p_B)\ \ [\bar{q}(x)\, q(x)]\ , \qquad \gamma_q = \frac{g_1^2}{2}\frac{m_q}{m_h^2} \tag{24}$$

where ϵ^μ are the $B^{(1)}$ polarization vectors, $q(x)$ is a quark field and there are separate couplings γ_q for each flavor of quark. g_1 is the hypercharge coupling, and $Y_h = 1/2$ has been explicitly included in the result. We have taken the non-relativistic (NR) limit for the WIMPs in which we are justified in dropping tiny terms of order $(p_B - p'_B)^2/m_h^2$. The factor of m_q in γ_q is a direct consequence of the fact that zero mode quark masses result from the quark couplings to Higgs, after electroweak symmetry breaking.

We now consider the KK quark exchange, with Feynman diagrams shown in Figure 3. Recall the coupling $B^{(1)}$-$q^{(1)}_{R(L)}$-q involves a right (left)-handed projector and both $q^{(1)}_R$ and $q^{(1)}_L$ can be exchanged and will typically have somewhat different masses. Thus each Feynman graph of Figure 3 is actually two separate graphs with $q^{(1)}_L$ and $q^{(1)}_R$ exchanged. The amplitudes corresponding to the two diagrams of Figure 3 are:

$$\mathcal{M}_1^{R/L} \;=\; -i(g_1 Y_{R/L})^2 \left[\overline{q}(x)\gamma^\nu P_{R/L}\frac{(\not{p}_q - \not{p}_{B'} + m_{q^{(1)}})}{(p_q - p_{B'})^2 - m^2_{q^{(1)}_{R/L}}}\gamma^\mu P_{R/L} q(x)\right] \epsilon^*_\mu(p'_B)\epsilon_\nu(p_B), \tag{25}$$

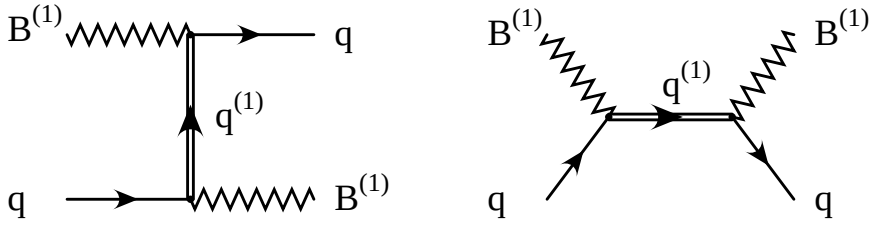

Figure 3: Leading Feynman graphs for effective $B^{(1)}$-quark scattering through the exchange of a KK quark. Both q^1_L and q^1_R should be understood in each graph.

$$\mathcal{M}_2^{R/L} = -i(g_1 Y_{R/L})^2 \left[\overline{q}(x)\gamma^\mu P_{R/L} \frac{(\not{p}_q + \not{p}_B + m_{q^{(1)}})}{(p_q+p_B)^2 - m^2_{q^{(1)}_{R/L}}} \gamma^\nu P_{R/L} q(x)\right] \epsilon^*_\mu(p_{B'})\epsilon_\nu(p_B), \quad (26)$$

where $Y_{R/L}$ are the hypercharges for the right- and left-chiral quark q. In the nonrelativistic limit $p_B \approx p_{B'} \approx (m_{B^{(1)}}, 0, 0, 0)$ so that $\mathcal{M}_q^{R/L} = \mathcal{M}_1^{R/L} + \mathcal{M}_2^{R/L}$ can be rewritten:

$$\begin{aligned}\mathcal{M}_q^{R/L} &= -ig_1^2 Y^2_{q_{R/L}} \epsilon^*_\mu(p_{B'})\ \epsilon_\nu(p_B) \times \quad (27)\\ &\quad \overline{q}(x)\left\{\frac{(E_q + m_{B^{(1)}})\gamma^\mu\gamma^0\gamma^\nu}{(m_{B^{(1)}}+E_q)^2 - m^2_{q^{(1)}}} + \frac{(E_q - m_{B^{(1)}})\gamma^\nu\gamma^0\gamma^\mu}{(m_{B^{(1)}}-E_q)^2 - m^2_{q^{(1)}}}\right\} P_{R/L}\ q(x)\ ,\end{aligned}$$

where we have neglected the 3-momentum of the quarks in the nucleon and written $p_q \approx (E_q, 0, 0, 0)$. $E_q < 1$ GeV $\ll M_{B^{(1)}}$ is the energy of a bound quark in the nucleon. We now expand this expression up to linear order in $x = E_q m_{B^{(1)}}/(m^2_{B^{(1)}} - m^2_{q^{(1)}})$ to obtain

$$\mathcal{M}_q^{R/L} = -i\epsilon^*_\mu(p_{B'})\ \epsilon_\nu(p_B)\overline{q}(x)\left[S_q E^{\mu\nu} + A_q \tilde{E}^{\mu\nu}\right] P_{R/L}\ q(x)\ , \quad (28)$$

where the coefficients S_q (scalar contribution) and A_q (spin-dependent contribution) are defined in equations (34) and

$$E^{\mu\nu} \equiv \gamma^\mu\gamma^0\gamma^\nu + \gamma^\nu\gamma^0\gamma^\mu\ , \quad \tilde{E}^{\mu\nu} \equiv \gamma^\mu\gamma^0\gamma^\nu - \gamma^\nu\gamma^0\gamma^\mu = 2i\epsilon^{0\mu\nu\rho}\gamma_\rho\gamma_5. \quad (29)$$

In the non relativistic limit $E^{\mu\nu}$ leads to scalar interactions whereas $\tilde{E}^{\mu\nu}$ leads to spin-dependent interactions.

We will assume that all flavors and chiralities of first level KK quarks are equal and parameterize their masses by $\Delta = (m_{q^{(1)}} - m_{B^{(1)}})/m_{B^{(1)}}$. Summing $\mathcal{M}_h$ and $\mathcal{M}_q^R + \mathcal{M}_q^L$ we obtain:

$$\langle\mathcal{M}\rangle = -i\epsilon^*_\mu(p_B)\ \epsilon_\nu(p_{B'})\left[(\gamma_q + S_q)g^{\mu\nu}\langle\overline{q}q\rangle + A_q\langle\overline{q}\tilde{E}^{\mu\nu}q\rangle\right], \quad (30)$$

$$|\langle\mathcal{M}_q\rangle|^2 = 4(\gamma_q + S_q)^2|\langle\overline{q}q\rangle|^2 + 2A_q^2|\langle\overline{q}\gamma^k\gamma_5 q\rangle|^2, \quad (31)$$

with,

$$\langle\overline{q}q\rangle = \frac{m_p}{m_q} f^p_{T_q}. \quad (32)$$

We sum over the different quark contributions to obtain the matrix element in a nucleon state. At this stage, as a first-order evaluation, we will make the assumption $E_q \approx m_q$. We recognize that the assumption that the light quarks in the nucleon are on-shell is questionable and that a more accurate treatment would be desirable[5].

For the spin matrix element only the light quarks u, d, s contribute while for the scalar matrix elements there are also contributions from heavy quarks c, b, t [18]:

$$f_{p,n}^{B^{(1)}} = m_{p,n} \sum_q \frac{\gamma_q + S_q}{m_q} f_{T_q}^{p,n}. \tag{33}$$

Because of this distinction, we drop terms in A_q which are proportional to any power of the zero mode quark mass since these are negligible. Note that under our assumption both γ_q and S_q are proportional to the quark mass m_q. Thus, given the normalization of the matrix elements f_{T_q}, each flavor contributes to the scalar interaction proportionally to its contribution to the nucleon mass. For heavy quarks $q = c, b, t$, the contribution should in fact be considered to be induced by the *gluon* content of the nucleon, with the heavy quark legs closed to form a loop. In the Higgs exchange case, the mapping from the tree graph with heavy quark external legs to the loop graph with external gluons is straight-forwardly handled by the formalism of [18]. For the KK quark graph, as emphasized in [19], this mapping is generally unreliable because of the presence of the heavy KK quark in the loop with mass $\sim m_{B^{(1)}}$. Thus, we include $q = c, b, t$ in γ_q, but to be conservative not in S_q. From a practical point of view, the loop-suppression renders the contribution from the heavy quarks irrelevant compared to the strange quark contribution, so the final results are insensitive to this choice of procedure.

The coefficients A_q and S_q may be extracted from the matrix elements,

$$\begin{aligned} A_q &= \frac{g_1^2 (Y_{q_L}^2 + Y_{q_R}^2) m_{B^{(1)}}}{(m_{B^{(1)}}^2 - m_{q^{(1)}}^2)}, \\ S_q &= -E_q \frac{g_1^2 (Y_{q_L}^2 + Y_{q_R}^2)}{(m_{B^{(1)}}^2 - m_{q^{(1)}}^2)^2} (m_{B^{(1)}}^2 + m_{q^{(1)}}^2). \end{aligned} \tag{34}$$

The total amplitude squared in a nucleus state reads:

$$|\langle \mathcal{M} \rangle|^2 = |\langle \mathcal{M} \rangle|_{scalar}^2 + |\langle \mathcal{M} \rangle|_{spin}^2 \,, \tag{35}$$

where,

$$|\langle \mathcal{M} \rangle|_{scalar}^2 = 4 m_N^2 (Z f_p^{B^{(1)}} + (A - Z) f_n^{B^{(1)}})^2 \times F_{sc}^2(|\mathbf{q}|), \tag{36}$$

$$|\langle \mathcal{M} \rangle|_{spin}^2 = \frac{32}{3} g_1^4 \frac{m_{B^{(1)}}^2 m_N^2}{(m_{B^{(1)}}^2 - m_{q^{(1)}}^2)^2} \Lambda^2 J(J+1) \times F_{sp}^2(|\mathbf{q}|), \tag{37}$$

[5] Note that this problem did not arise in the elastic scattering of a neutralino because neutralinos can only exchange bosons when interacting with spin-1/2 quarks. On the other hand, our bosonic dark matter candidate can exchange fermions with the quarks. This interaction involves fermion propagator and therefore involves the energy, and not only the mass, of the quark. Possibly the use of a constituent mass might be more appropriate in this case.

so that the corresponding cross sections at zero momentum transfer, σ_0 are,

$$\sigma_0^{scalar} = \frac{m_N^2}{4\pi(m_{B^{(1)}}+m_N)^2}(Zf_p^{B^{(1)}}+(A-Z)f_n^{B^{(1)}})^2, \quad (38)$$

$$\sigma_0^{spin} = \frac{2}{3\pi}\mu^2 g_1^4 \frac{\Lambda^2 J(J+1)}{(m_{B^{(1)}}^2-m_{q^{(1)}}^2)^2}. \quad (39)$$

where,

$$\Lambda = \frac{a_p\langle S_p\rangle + a_n\langle S_n\rangle}{J}, \quad (40)$$

and,

$$a_{p(n)} = \sum_{u,d,s}(Y_{q_L}^2+Y_{q_R}^2)\Delta^{p(n)}q. \quad (41)$$

Using $\Delta^{(n)}u = \Delta^{(p)}d \equiv \Delta d$, $\Delta^{(n)}d = \Delta^{(p)}u \equiv \Delta u$ and $\Delta^{(n)}s = \Delta^{(p)}s \equiv \Delta s$, we have,

$$a_p = \frac{17}{36}\Delta u + \frac{5}{36}(\Delta d + \Delta s), \quad (42)$$

$$a_n = \frac{17}{36}\Delta d + \frac{5}{36}(\Delta u + \Delta s), \quad (43)$$

where $\Delta u = 0.78 \pm 0.02$, $\Delta d = -0.48 \pm 0.02$, and $\Delta s = -0.15 \pm 0.02$ [20]. For the spin form factors we will also need the iso-singlet and iso-vector combinations,

$$a_0 = \frac{11}{18}(\Delta u + \Delta d) + \frac{5}{18}\Delta s, \quad (44)$$

$$a_1 = \frac{1}{3}(\Delta u - \Delta d). \quad (45)$$

For Germanium and Iodine nuclei we have, assuming the WIMP mass is 1 TeV, $\Delta = (m_{q^{(1)}} - m_{B^{(1)}})/m_{B^{(1)}} = 15\%$, and the Higgs mass is $m_h = 120$ GeV,

$$\text{Germanium} : \sigma_0^{scalar} = 1.6\times 10^{-3}\text{ pb}, \quad \sigma_0^{spin} = 1.4\times 10^{-4}\text{ pb}, \quad (46)$$

$$\text{Iodine} : \sigma_0^{scalar} = 1.34\times 10^{-2}\text{ pb}, \quad \sigma_0^{spin} = 1.8\times 10^{-3}\text{pb}. \quad (47)$$

These values are somewhat smaller than what one would typically expect for neutralino-nucleus elastic scattering. In that case, one finds [14],

$$\sigma_{0,\chi}^{scalar} \simeq \frac{4\mu^2}{\pi}(Zf_p^\chi + (A-Z)f_n^\chi)^2 \quad , \quad (48)$$

$$\sigma_{0,\chi}^{spin} \simeq \frac{32}{\pi}G_F^2\mu^2\Lambda^2 J(J+1), \quad (49)$$

so that,

$$\frac{\sigma_{0,B^{(1)}}^{scalar}}{\sigma_{0,\chi}^{scalar}} \sim \frac{1}{16m_{B^{(1)}}^2}\left(\frac{f_p^{B^{(1)}}}{f_p^\chi}\right)^2. \quad (50)$$

Using $f_p = m_p \sum f_{T_q} f_q / m_q$ where $f_q^{B^{(1)}} \sim \gamma_q$ and $f_q^{\chi} \sim g_2 T_{h00}\, h_{hqq}/2m_h^2$ (note that $f_q^{B^{(1)}}$ and f_q^{χ} have different dimensions) where T_{h00} and h_{hqq} are Higgs-neutralino-neutralino and Higgs-quark-quark Yukawa couplings (which can be found, for instance, in Ref. [14]), we have,

$$\frac{\sigma^{scalar}_{0,B^{(1)}}}{\sigma^{scalar}_{0,\chi}} \sim \left(\frac{g_1}{g_2}\right)^4 \left(\frac{m_W}{m_{B^{(1)}}}\right)^2 \sim 10^{-3}, \tag{51}$$

Therefore we expect $\sigma^{scalar}_{0,\chi}$ to be smaller than $\sigma^{scalar}_{0,B^{(1)}}$, however the ratio generally depends on the precise neutralino couplings, which are complicated functions of SUSY parameter space. We now compare spin-dependent cross sections:

$$\frac{\sigma^{spin}_{0,B^{(1)}}}{\sigma^{spin}_{0,\chi}} \propto \frac{g_1^4}{48}\left(\frac{a_p^{B^{(1)}}}{a_p^{\chi}}\right)^2 \frac{1}{G_F^2 (m_{B^{(1)}} - m_{q^{(1)}})^2} \sim \left(\frac{g_1}{g_2}\right)^4 \frac{m_W^4}{(m^2_{B^{(1)}} - m^2_{q^{(1)}})^2}. \tag{52}$$

We again have a large suppression factor due to the large WIMP mass unless $m_{q^{(1)}}$ is nearly degenerate with $m_{B^{(1)}}$.

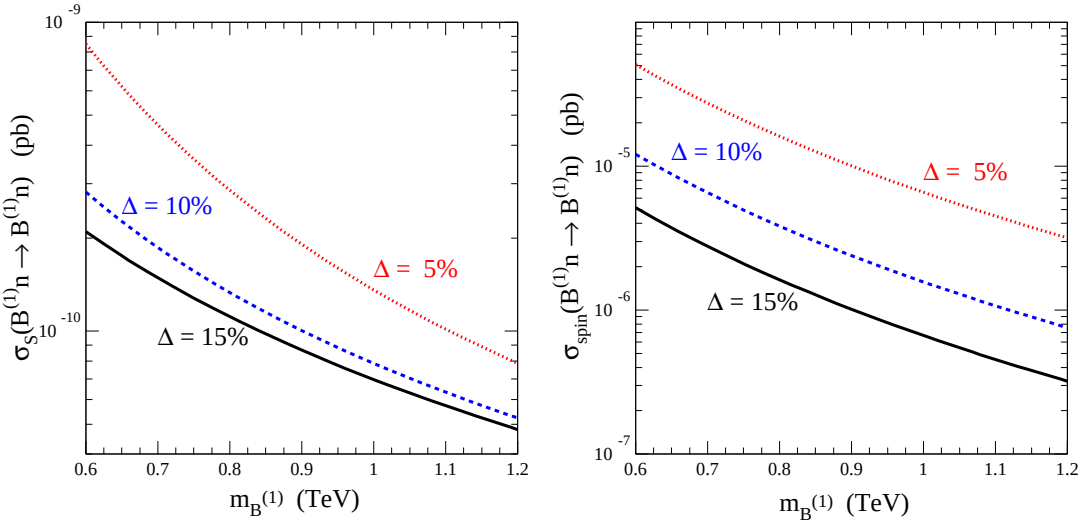

Figure 4: Spin-dependent and spin-independent WIMP-nucleon cross sections as a function of the WIMP mass for (top to bottom) $\Delta = (m_{q^{(1)}} - m_{B^{(1)}})/m_{B^{(1)}} = 5, 10, 15\%$ and $m_h = 120$ GeV.

It is common for dark matter search experiments to express their constraints in terms of effective WIMP-nucleon cross sections,

$$\sigma^{spin}_{p,n} = \frac{g_1^4}{2\pi}\frac{\mu^2_{p,n} a^2_{p,n}}{(m^2_{B^{(1)}} - m^2_{q^{(1)}})^2}, \tag{53}$$

$$\sigma^{scalar}_{p,n} = \sigma_0 \frac{m^2_{p,n}}{\mu^2}\frac{1}{A^2}. \tag{54}$$

For 1 TeV WIMP mass, typical values are $\sigma_{p,n}^{scalar} \sim 10^{-10}$ pb and $\sigma_{p,n}^{spin} \sim 10^{-6}$ pb. (For comparison, nucleon-neutralino cross sections are in the range $10^{-12} - 10^{-6}$ pb for scalar interactions and $10^{-9} - 10^{-4}$ pb for spin-dependent interactions). ¿From Fig. 5 we see that the cross sections may vary upward by about one order of magnitude if $m_{B^{(1)}}$ is at the lower end of its favored range, 600 GeV, and by two orders of magnitude if in addition $B^{(1)}$ and $q^{(1)}$ are more degenerate, $\Delta \sim 5\%$. The dependence on the zero-mode Higgs mass is presented in Fig. 5. Note that theories in which the top and/or bottom quarks propagate in extra dimensions [21] generically have additional contributions to electroweak observables through the oblique parameters S and T [4], and thus the preference in the precision electroweak data for a light SM-like Higgs may be misleading in theories with universal extra dimensions. Thus, we consider a wider range of Higgs masses than one would naively expect from the electroweak fits. Finally, in Fig. 6, we show a scatter plot of spin-dependent and spin-independent cross sections, varying 600 GeV $\leq m_{B^{(1)}} \leq$ 1200 GeV, $5\% \leq \Delta \leq 15\%$, and 100 GeV $\leq m_h \leq$ 200 GeV.

In any case, these cross sections are below the reach of any currently running experiment. However, larger mass detectors composed of heavier nuclei and improved efficiencies will most likely change this situation in the foreseeable future. Since precise event rates will depend on experimental issues such as efficiencies and background rates and rejection, it is important to include nuclear effects in the theoretical predictions, and worthwhile to study kinematic distributions such as dR/dE_r.

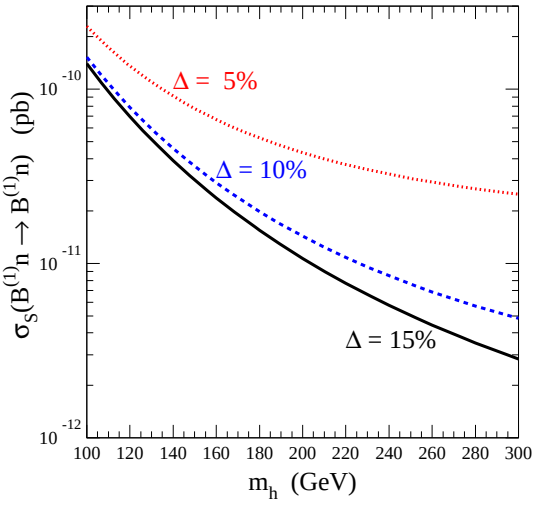

Figure 5: Scalar WIMP-nucleon cross section as a function of the Higgs mass for $m_{B^{(1)}} = 1$ TeV and (top to bottom) $\Delta = (m_{q^{(1)}} - m_{B^{(1)}})/m_{B^{(1)}} = 5, 10, 15\%$.

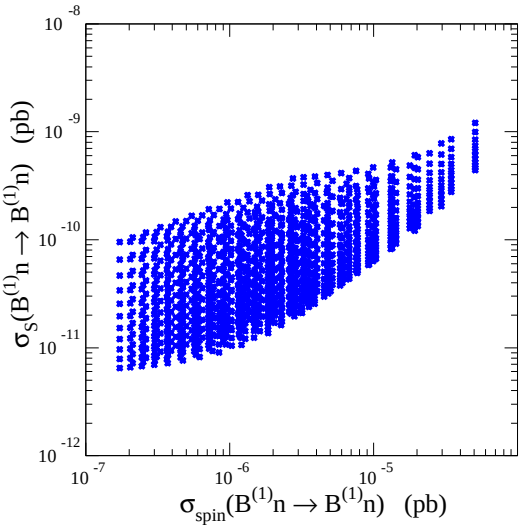

Figure 6: Predictions for $B^{(1)}$-nucleon cross sections in the spin-independent – spin-dependent plane. We have varied three parameters: $m_{B^{(1)}}$ in the 600-1200 GeV range, Δ in the 5-15 % range and m_h in the 100-200 GeV range.

5 Differential and Integrated Event Rates

From Eq. (9), the number of events per kilogram of detector per keV per day is proportional to,

$$\frac{dR}{dE_r} \propto \frac{\sigma_0}{m\mu^2} F^2(|\mathbf{q}|). \tag{55}$$

Larger m and smaller σ_0 combine with a suppression from $F^2(|\mathbf{q}|)$, making the event rate quite low. The rates are further suppressed by nuclear form factors which drop quickly as the recoil energy increases.

Nucleus-A	Typical Recoil Momentum $\mathbf{q} = \mu v$	Typical Recoil Energy $\lvert\mathbf{q}\rvert^2/2M$
Silicon-23	22 MeV	11 keV
Sodium-29	28 MeV	14 keV
Germanium-73	68 MeV	32 keV
Iodine-127	112 MeV	50 keV
Xenon-131	116 MeV	51 keV

Table 1: Typical nucleus recoil momenta and energies after scattering with a WIMP with mass $m \gg M$.

In Table 1 we list some typical recoil momenta and energies (corresponding to a WIMP mass of 1 TeV and velocity of $v \sim 220$ km/s $\sim 10^{-3}c$) scattering from various nuclei. Note that there is effectively a maximal recoil energy which is roughly 16 times the typical recoil energy listed in the table, because the maximum velocity is approximately the galactic escape velocity, $v_{esc} = 650 \pm 200$ km/s $\sim 2v$ and $q_{max} = 2\mu v_{max}$. However, at such energies the nuclear form factor itself already provides a high suppression in the differential rate, such that one arrives at a good approximation to the integrated rate by integrating up to an energy which is four times the typical energy. Thus, it is enough for our purposes to present dR/dE_r over a 200 keV range of recoil energy. Experimentally, it may be useful to look at energies $\gtrsim 100$ keV for which we expect the background to fall off. We illustrate the importance of nuclear effects in Fig. 7 where we plot the scalar and spin form factors for ı127, as a function of the WIMP mass. We can see that they lead, for a 1 TeV WIMP, to a suppression of the cross section by a factor of approximately 15.

We now examine the differential rate with respect to recoil energy for several materials. This distribution is important in order to correctly apply experimental efficiencies as well as to assess signal-to-background levels as a function of the cut on the recoil energy, E_r^{min}. In Fig. 8 we present the predictions for rates differential in recoil energy on three different targets: NaI, ^{73}Ge, and ^{131}Xe, including both spin-dependent and scalar contributions along with appropriate nuclear effects. For scalar contributions, this is the form factor given in Eq. (10). For spin-dependent form factors, we use those presented in [22] for

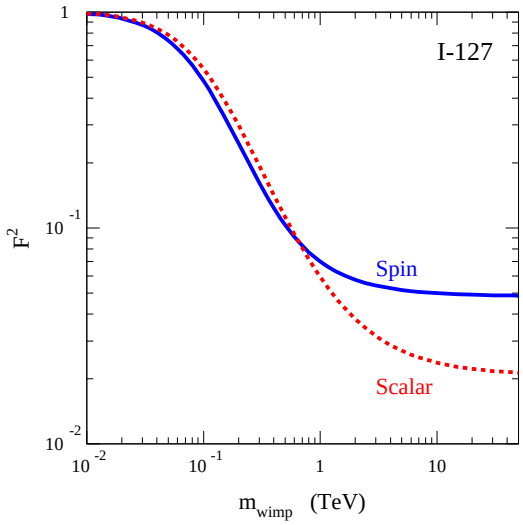

Figure 7: Spin and scalar nuclear form factors for Iodine as a function of the WIMP mass. Note that form factors are usually expressed as a function of the recoil energy $E_r = \mathbf{q}^2/2M$. To generate this plot, we chose a typical recoil momentum $\mathbf{q} = \mu v$ so that $E_r(m) = m^2 v^2 M/(2(m+M)^2)$.

^{73}Ge. For Iodine, Sodium and ^{131}Xe, we adopt the spin form factors of [23] estimated by considering the Nijmegen (II) nucleon-nucleon potential.

In order to obtain the observable rates at detectors, we integrate the differential cross sections over the recoil energies to which they are sensitive. The minimum observable energy is a function of the experimental set-up and background levels. In Table 2 we present some current and near-future dark matter search experiments, including their primary target nucleus, target mass, and an estimation of the minimum recoil energy required for an observable event. For the NaI detectors, we have included DAMA (100 kg of NaI) and LIBRA (an upgrade of DAMA: 250 kg of NaI) [24]. There are also several different detectors based on various isotopes of Germanium. The first stage of GENIUS is composed of 100 kg of ^{73}Ge, whereas the second stage consists of between 100-10000 kg of a mixture of 86% ^{76}Ge and 14% ^{74}Ge [25]. The MAJORANA experiment will search for double-beta-decay with 500 kg of the same mixture of 86% ^{76}Ge and 14% ^{74}Ge [26]. Finally, the proposed XENON experiment will consist of 1000 kg of ^{131}Xe [27].

In Fig. 9 we show the potential number of events per year at detectors based on Germanium isotopes, assuming E_r^{min} is 11 keV. The bands represent potential signal rates as a function of the LKP mass, varying $5\% \leq \Delta \leq 15\%$ and 115 GeV $\leq m_h \leq$ 200 GeV. To illustrate the importance of large mass detectors, we have chosen to compare the 100 kg ^{73}Ge GENIUS, 10^4 kg ^{76}Ge and ^{74}Ge GENIUS stage II, and 500 kg ^{76}Ge and ^{74}Ge MAJORANA experiments. Evident from the figure, in order to have even one event

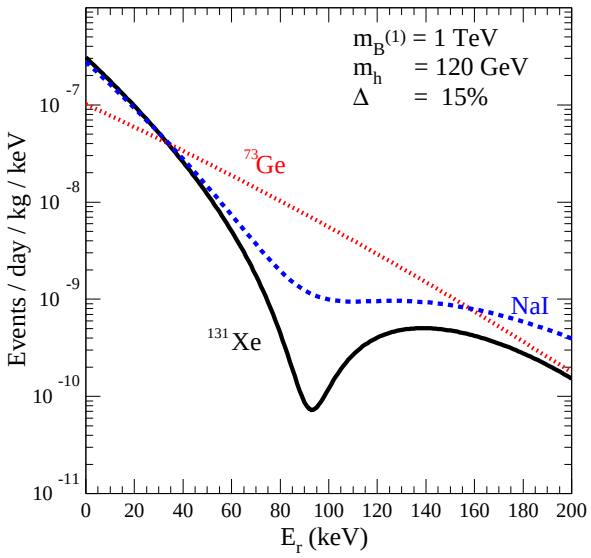

Figure 8: Energy Spectrum of events for three types of detectors: ^{73}Ge (dotted curve), NaI (dashed curve) and ^{131}Xe (solid curve) for $m_{B^{(1)}} = 1$ TeV, m_h=120 GeV and $\Delta = 15\%$.

per year at GENIUS or MAJORANA, m_h and Δ must be on the small side of the band, and/or $m_{B^{(1)}}$ must be less than about 1 TeV. In order to have ten or more events per year, at MAJORANA, we must have $m_{B^{(1)}} \leq 700$ GeV as well as small m_h and Δ. Thanks to its enormous mass, the upgraded GENIUS experiment with 10^4 kg of ^{76}Ge and ^{74}Ge can do much better, with more than ten events per year when $m_{B^{(1)}} \leq 700$ GeV even for unfavorable m_h and Δ, and more than ten events over the entire range of $m_{B^{(1)}}$ for optimal m_h and Δ.

In Fig. 10 we show events per year, varying the parameters as above at DAMA and DAMA/LIBRA. DAMA, with 100 kg of NaI can observe more than ten events per year if the LKP is light and parameters favorable. DAMA/LIBRA, with 250 kg of NaI can observe the lightest relevant LKP masses even when Δ and m_h are at the larger end we consider. Finally, the XENON experiment combines a heavy ^{131}Xe target with a large 1000 kg detector. The estimated events per year are plotted in Fig. 11, and are comparable to the end-stage of GENIUS II with 10^4 kg of Germanium. For comparable masses, XENON could in fact do better, thanks to the heavier target nucleus.

Our results indicate that to directly detect Kaluza-Klein dark matter, heavy target nuclei and large mass detectors are essential. Of course, the actual reach of the experiments will depend on experimental issues such as efficiencies and backgrounds, which are beyond the scope of this work. However, given the relatively large event rates which are possible at planned experiments, further detailed study of this subject is warranted.

Experiment	Target	Mass	E_r^{min}
DAMA	NaI	100 kg	20 keV
DAMA/LIBRA	NaI	250 kg	20 keV
GENIUS	^{73}Ge	100 kg	11 keV
GENIUS II	^{76}Ge, ^{74}Ge	100-10000 kg	11 keV
MAJORANA	^{76}Ge, ^{74}Ge	500 kg	11 keV
XENON	^{131}Xe	1000 kg	4 keV

Table 2: Present and near-future dark matter detection experiments.

6 Conclusion

The identity of the dark matter is one of the most intriguing puzzles in modern physics, and has sparked a major experimental program to search for these elusive objects. In fact, one of the primary motivations of the supersymmetric standard model (with R-parity) is the fact that it has a natural WIMP candidate. However, we have recently seen that a large class of extra-dimensional models with a KK parity also provides a natural WIMP - the heavy Kaluza-Klein modes of the ordinary photon and Z boson. While KK parity is not a necessary feature of models with extra dimensions (just as R-parity is an unnecessary feature of models with supersymmetry), it can be imposed self-consistently in the low energy effective theory. Estimates of the relic density indicate that such particles should have masses at the TeV scale, at the frontier of current collider and direct detection searches.

In this article we have made a detailed study of the direct detection of LKPs which scatter off of heavy nuclei. Subject to our assumptions that boundary terms are small (perhaps generated radiatively) and common for all quarks, our predictions depend on three parameters: the LKP mass, the splitting between the LKP and the first level KK quarks, and the mass of the zero-mode Higgs. The mixture of KK B and W_3 in the LKP is another parameter, which would also be interesting to study in more detail. This situation is to be contrasted with the minimal supersymmetric standard model, which requires four parameters to describe the neutralino alone. We find that nuclear effects are important to include in the cross sections, particularly because of the heavy WIMP masses favored by the estimates of the relic density. These effects render rates at current dark matter searches small, and indicate that future experiments composed of large numbers of heavy nuclei can study most, but not all of the parameter space relevant for the correct WIMP relic density.

Another search strategy which we have not considered here relies on indirect detection, in which WIMPs annihilate one another producing energetic photons and positrons [9,11] or neutrinos [9, 10, 11] which can be observed on the Earth. The resulting LKP masses

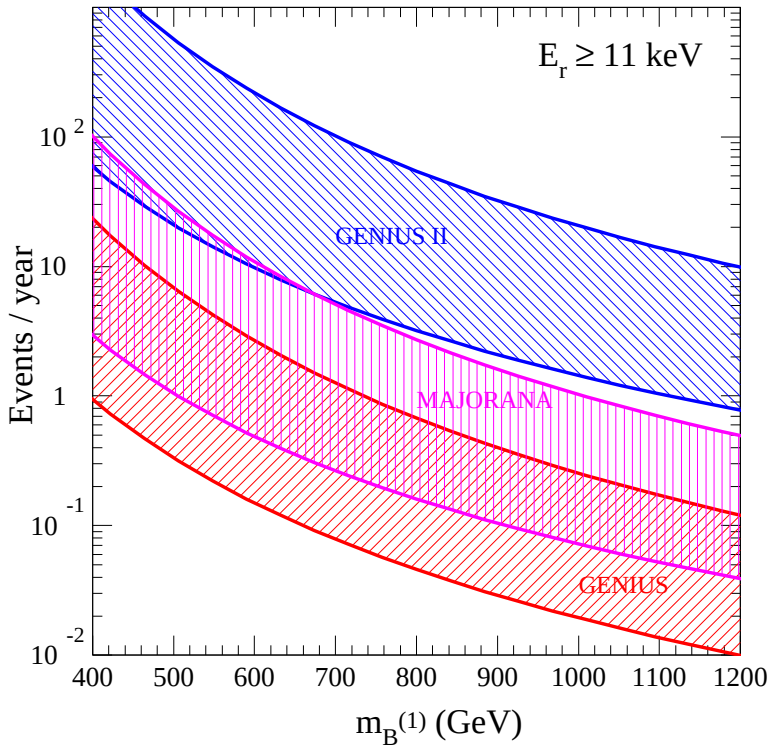

Figure 9: Number of events per year for the 100 kg ^{73}Ge Genius experiment, the 10^4 kg ^{76}Ge/^{74}Ge GENIUS stage II, and 500 kg ^{76}Ge/^{74}Ge MAJORANA experiment. The bands are obtained by varying $5\% \leq \Delta \leq 15\%$ and 115 GeV $\leq m_h \leq$ 200 GeV.

which can be probed by next-generation experiments are similar to those determined here from planned direct searches such as GENIUS.

In conclusion, Kaluza-Klein dark matter is well-motivated in a large class of theories with compact extra dimensions, and provides an interesting alternative to the standard neutralino LSP in a supersymmetric model. Accurate determination of scattering cross sections with heavy nuclei involve nuclear form factors, and indicate that future experiments can study a significant region of parameter space. At the same time, collider searches at the Tevatron Run II and LHC will study a similar range of parameter space. The exciting scenario of KK dark matter can be studied on two fronts simultaneously in the near future.

Acknowledgments

We are grateful to John Beacom, Hsin-Chia Cheng, Juan Collar and Neil Weiner for discussions. We thank the hospitality of the Aspen Center for Physics as well as the T-8 group of Los Alamos National laboratory for the Santa Fe Institute 2002 where part of this work was completed. This work is supported in part by the US Department of Energy, High Energy Physics Division, under contract W-31-109-Eng-38 and also by the David and Lucile Packard Foundation. Fermilab is operated by Universities Research Association Inc. under contract no. DE-AC02-76CH02000 with the DOE.

References

[1] G. Servant and T. M.P. Tait, arXiv:hep-ph/0206071. In press (Nucl. Phys. B).

[2] K. R. Dienes, E. Dudas and T. Gherghetta, Nucl. Phys. B **537**, 47 (1999) [arXiv:hep-ph/9806292].

[3] H. C. Cheng, K. T. Matchev and M. Schmaltz, arXiv:hep-ph/0205314.

[4] T. Appelquist, H. C. Cheng and B. A. Dobrescu, Phys. Rev. D **64**, 035002 (2001) [arXiv:hep-ph/0012100].

[5] H. Georgi, A. K. Grant and G. Hailu, Phys. Lett. B **506**, 207 (2001) [arXiv:hep-ph/0012379].

[6] H. C. Cheng, K. T. Matchev and M. Schmaltz, arXiv:hep-ph/0204342.

[7] M. Carena, T. M.P. Tait and C.E.M. Wagner, arXiv:hep-ph/0207056.

[8] I. Antoniadis, Phys. Lett. B **246**, 377 (1990).

[9] H. C. Cheng, J. L. Feng and K. T. Matchev, arXiv:hep-ph/0207125.

[10] D. Hooper and G. D. Kribs, arXiv:hep-ph/0208261.

[11] G. Bertone, G. Servant and G. Sigl, arXiv:hep-ph/0211342.

[12] M. W. Goodman and E. Witten, Phys. Rev. D **31**, 3059 (1985).

[13] E. I. Gates, G. Gyuk and M. S. Turner, Astrophys. J. **449**, L123 (1995) [arXiv:astro-ph/9505039].

[14] G. Jungman, M. Kamionkowski and K. Griest, Phys. Rept. **267**, 195 (1996) [arXiv:hep-ph/9506380].

[15] J. Engel, S. Pittel and P. Vogel, Int. J. Mod. Phys. E **1**, 1 (1992).

[16] D. Abrams *et al.* [CDMS Collaboration], arXiv:astro-ph/0203500.

[17] A. Benoit *et al.* [EDELWEISS Collaboration], Phys. Lett. B **513**, 15 (2001) [arXiv:astro-ph/0106094].

[18] M. A. Shifman, A. I. Vainshtein and V. I. Zakharov, Phys. Lett. B **78**, 443 (1978).

[19] M. Drees and M. Nojiri, Phys. Rev. D **48**, 3483 (1993) [arXiv:hep-ph/9307208].

[20] J. R. Ellis, A. Ferstl and K. A. Olive, Phys. Lett. B **481**, 304 (2000) [arXiv:hep-ph/0001005].

[21] For some well-motivated examples which fit naturally in the UED framework: H. C. Cheng, B. A. Dobrescu and C. T. Hill, Nucl. Phys. B **589**, 249 (2000) [arXiv:hep-ph/9912343]; N. Arkani-Hamed, H. C. Cheng, B. A. Dobrescu and L. J. Hall, Phys. Rev. D **62**, 096006 (2000) [arXiv:hep-ph/0006238]; H. J. He, C. T. Hill and T. M.P. Tait, Phys. Rev. D **65**, 055006 (2002) [arXiv:hep-ph/0108041].

[22] V. Dimitrov, J. Engel and S. Pittel, Phys. Rev. D **51**, 291 (1995) [arXiv:hep-ph/9408246].

[23] M. T. Ressell and D. J. Dean, Phys. Rev. C **56**, 535 (1997) [arXiv:hep-ph/9702290].

[24] R. Bernabei *et al.*, arXiv:astro-ph/0205047.

[25] H. V. Klapdor-Kleingrothaus, arXiv:hep-ph/0104028.

[26] C. E. Aalseth *et al.* [Majorana Collaboration], arXiv:hep-ex/0201021.

[27] E. Aprile *et al.*, arXiv:astro-ph/0207670.

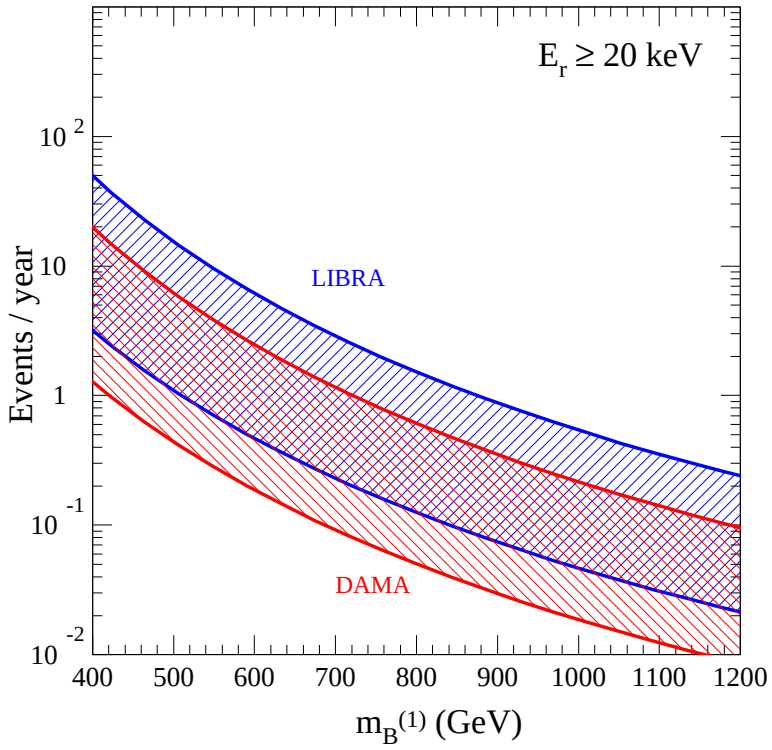

Figure 10: Number of events per year for the 100 kg NaI DAMA experiment, and 250 kg NaI DAMA/LIBRA experiment. The bands are obtained by varying $5\% \leq \Delta \leq 15\%$ and 115 GeV $\leq m_h \leq$ 200 GeV. Note that a signal in a DAMA-like experiment is not given by the number of WIMP-nucleus scattering events; rather, it is the annual modulation of this event rate, which amounts to a small fraction of the signal rate. Experiments of this kind use a different methodology as they do not attempt to distinguish between signal and background on an event-by-event basis. Our figure should then be interpreted as a theorist prediction of the number of events 100 kg and 250 kg NaI detectors can detect per year. In the particular case of the DAMA/LIBRA experiment, the amplitude of the modulation must scale like the total rate.

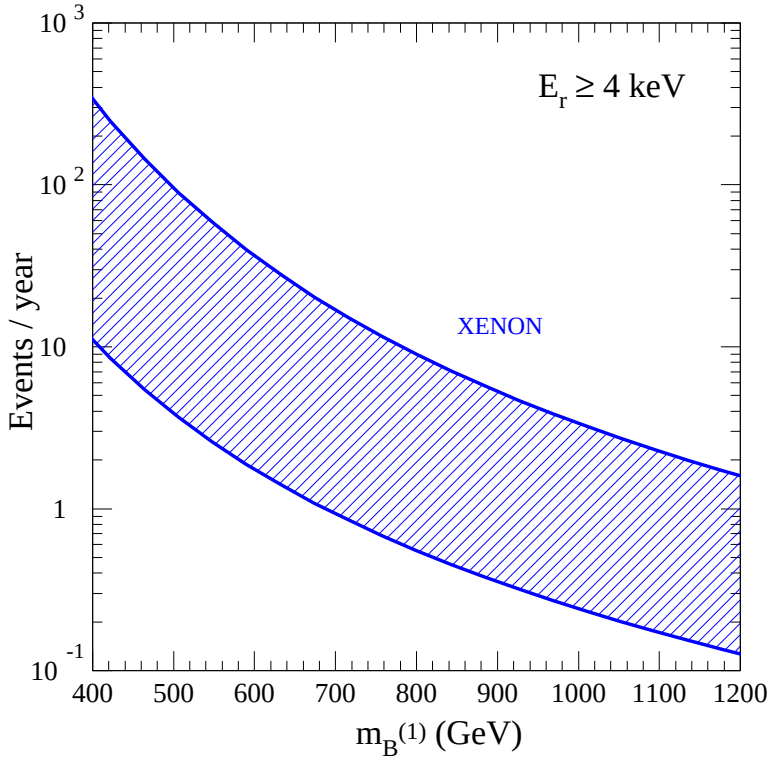

Figure 11: Number of events per year for the 1000 kg ^{131}Xe XENON experiment. The bands are obtained by varying $5\% \leq \Delta \leq 15\%$ and 115 GeV $\leq m_h \leq$ 200 GeV.